SUPPORTING INFORMATION

Learning from Correlations Based on Local Structure: Rare-earth Nickelates Revisited

Nicholas Wagner, Danilo Puggioni, and James M. Rondinelli*

Department of Materials Science and Engineering, Northwestern University, Illinois 60208-3108, USA

E-mail: jrondinelli@northwestern.edu

Scatter Matrices

Scatter plots of the amplitude and ordering temperatures from the experiment and DFT structure data sets.

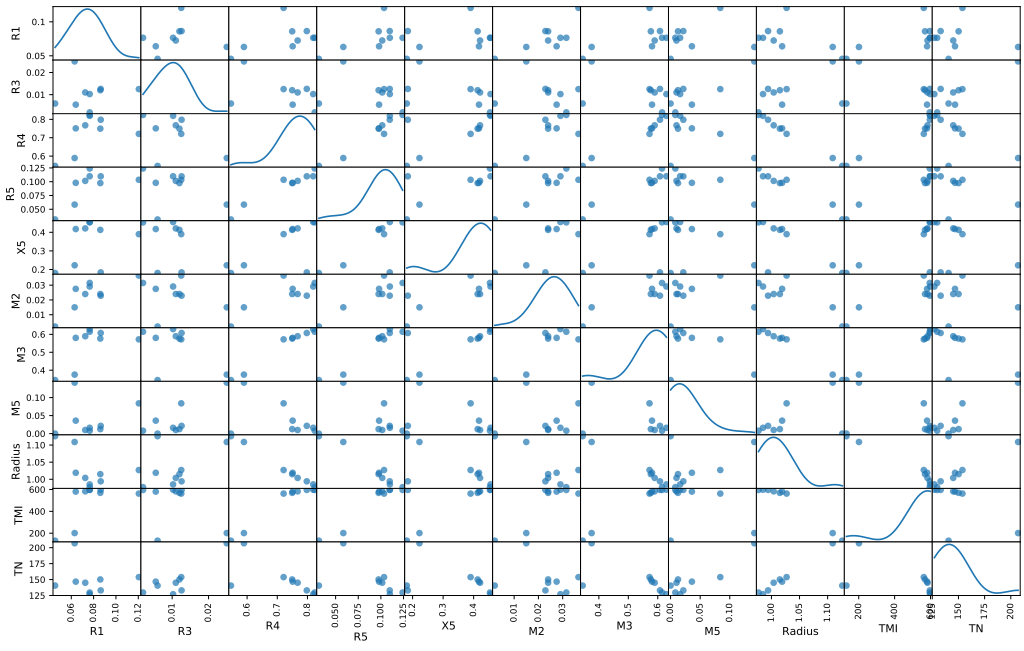

Figure S1: Scatter plot matrix from experiment using distortion-mode amplitudes. The diagonal elements are kernel density estimations for each variable.

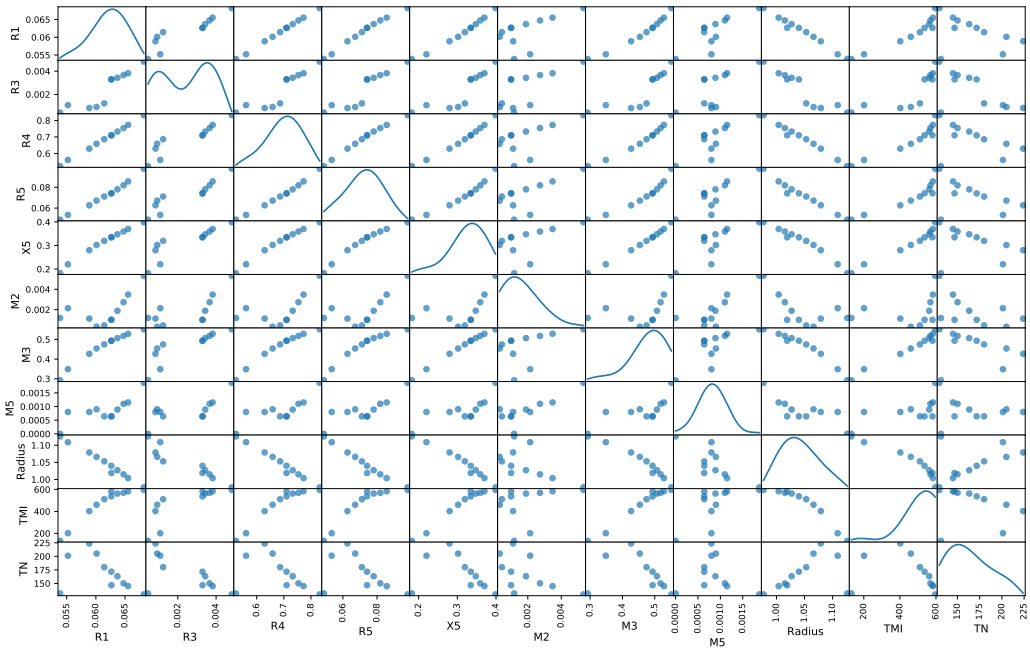

Figure S2: Scatter plot matrix from DFT using distortion-mode amplitudes. The diagonal elements are kernel density estimations for each variable.

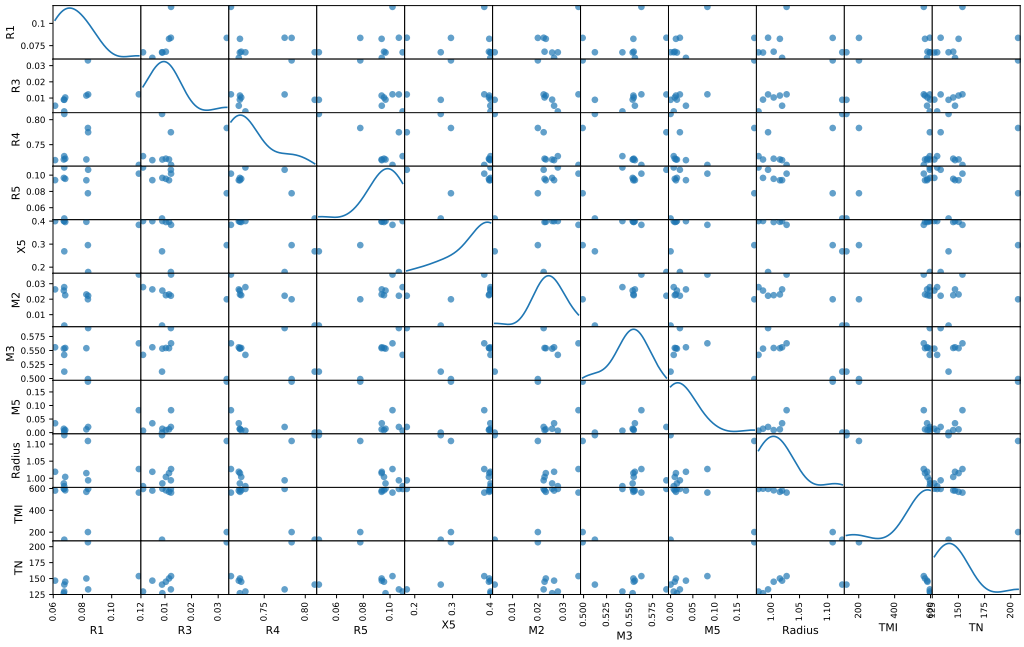

Figure S3: Scatter plot matrix from experiment using normalized distortion-mode amplitudes. The diagonal elements are kernel density estimations for each variable.

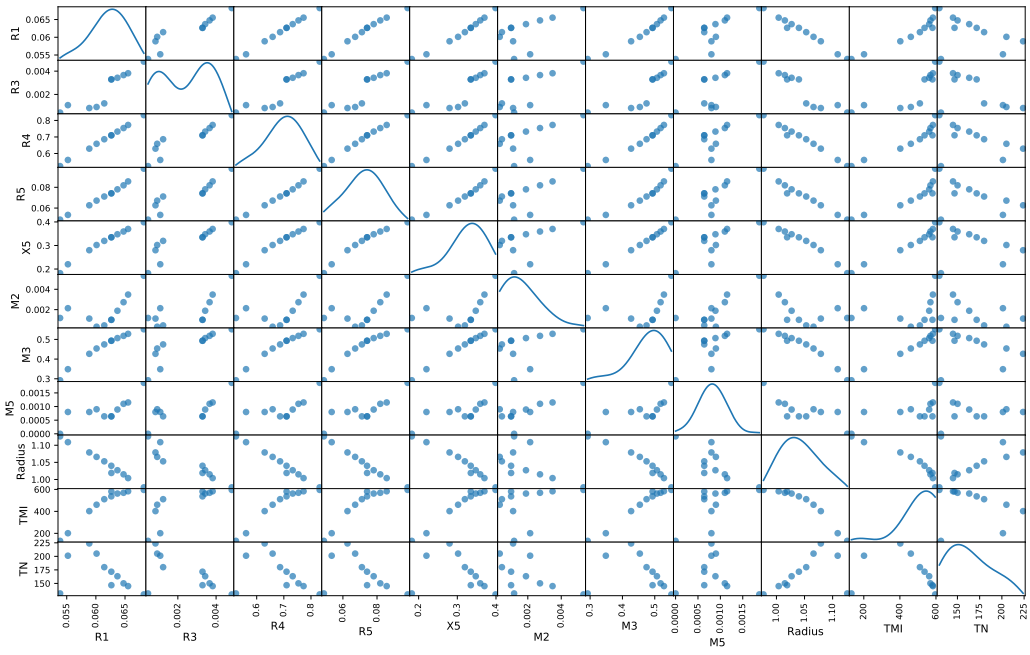

Figure S4: Scatter plot matrix from DFT using normalized distortion-mode amplitudes. The diagonal elements are kernel density estimations for each variable.

Normalized Correlation-Coefficient-Heat Map for Experimental Structures

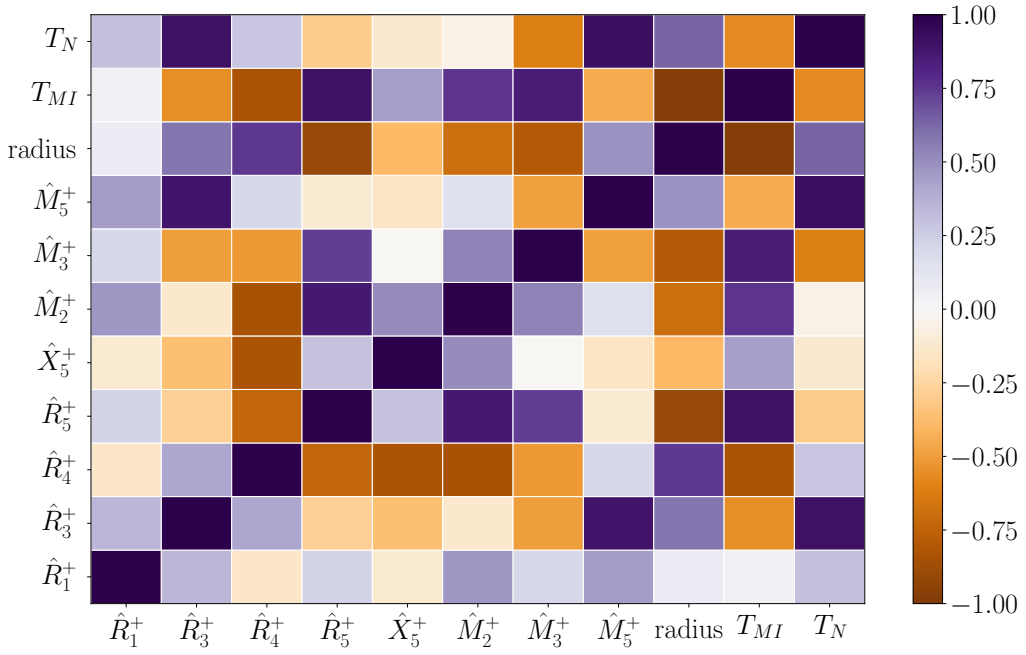

Figure S5: Normalized correlation-coefficient-heat maps (*n*CCHMs) calculated from the experimentally published crystal structures. Normalization is indicated by a 'hat' on the irrep label and is based on the Euclidean norm of the total mode vector mapping $Pm\bar{3}m \rightarrow P2_1/c$. All ordering temperatures correspond to values from experiment.

Distortion Modes for $NdNiO_3$

Table S1 provides the distortion mode amplitudes given with respect to the $Pm\bar{3}m$ aristotype based on the experimental and our DFT calculated $P2_1/c$ $NdNiO_3$ structures. We also provide the metric, ξ, defined as the ratio between the DFT and experimental amplitude of each irreducible representation (irrep) in the correct antiferromagnetic E' (AFM-E′) spin order. The breathing (R_1^+), a-type Jahn-Teller (R_3^+), and rumpling M_5^+) distortions responsible for the $Pnma \rightarrow P2_1/c$ symmetry lowering transition are shown in bold. The physical representation of each distortion mode is presented in Fig. 1 of the main text.

Table S1: Distortion modes for the theoretical (DFT) and experimental low temperature phase of $NdNiO_3$ (in units of Å).

$NdNiO_3$	$\mathbf{R_1^+}$	$\mathbf{R_3^+}$	R_4^+	R_5^+	M_2^+	M_3^+	$\mathbf{M_5^+}$	X_5^+
AFM-E′ (DFT)	**0.062**	**0.001**	0.581	0.057	0.002	0.366	**0.0004**	0.237
Experiment (Ref. 1)	**0.063**	**0.025**	0.589	0.059	0.015	0.375	**0.141**	0.222
ξ	**0.98**	**0.04**	0.99	0.97	0.13	0.98	**0.003**	1.07

Table S2 provides the distortion mode amplitudes given with respect to the $Pm\bar{3}m$ aristotype based on the the experimental *Pnma* $NdNiO_3$ structures reported at 293K. For each mode, we provide the coefficient of variation, which is defined as the standard deviation divided by the mean.

Table S2: Distortion modes for the experimental high temperature phase of $NdNiO_3$ (in units of Å) and the coefficient of variation (last column) for five different ICSD reports specified by collection code (CC) in the first row.

Mode	CC:164562	CC:78319	CC:24875	CC:69788	CC:67725	Coeff. of Var.
R_4^+	0.537	0.503	0.685	0.53557	0.554	0.113
R_5^+	0.047	0.091	0.143	0.04614	0.038	0.544
X_5^+	0.193	0.353	0.263	0.197	0.189	0.264
M_2^+	0.038	0.024	0.011	0.010	0.0043	0.690
M_3^+	0.371	0.342	0.441	0.398	0.373	0.087

References

(1) Garcia-Muñoz, J. L.; Aranda, M. A. G.; Alonso, J. A.; Martinez-Lope, M. J. Structure and Charge Order in the Antiferromagnetic Band-Insulating Phase of $NdNiO_3$. *Phys. Rev. B* **2009**, *79*, 134432.